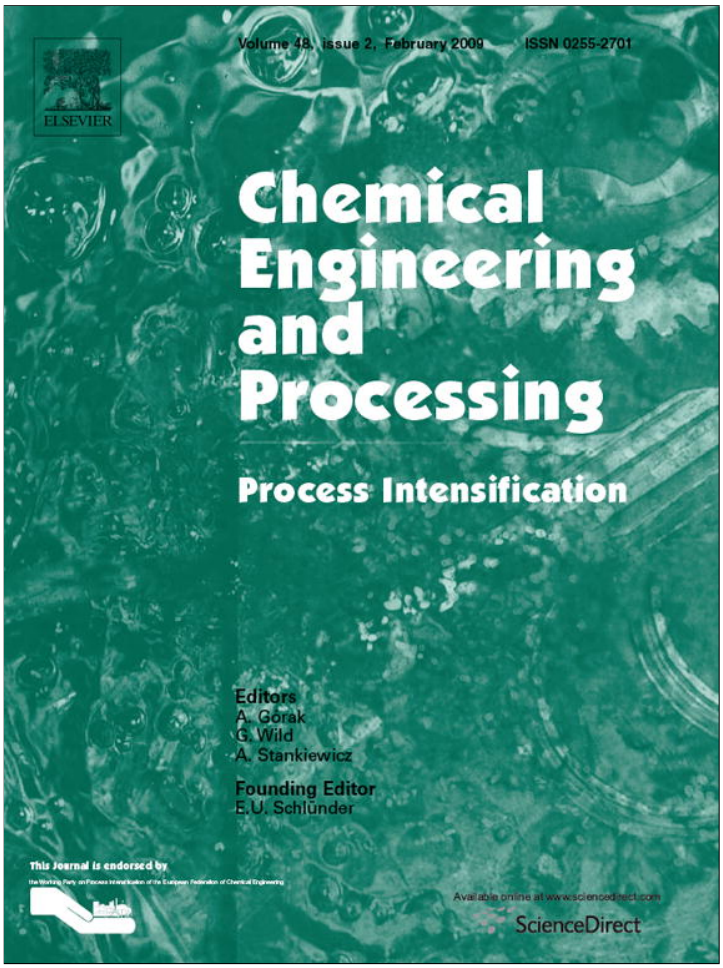

Chemical Engineering and Processing 48 (2009) 633–642

Contents lists available at ScienceDirect

Chemical Engineering and Processing: Process Intensification

journal homepage: www.elsevier.com/locate/cep

Dispersion of silicone oil in water surfactant solution: Effect of impeller speed, oil viscosity and addition point on drop size distribution

Amer EL-Hamouz[a,*], Mike Cooke[b], Adam Kowalski[c], Paul Sharratt[b]

[a] Department of Chemical Engineering, An-Najah National University, Nablus, West Bank, P.O. Box 7, The Palestinian Authority, Occupied Palestinian Territory
[b] School of Chemical Engineering and Analytical Science, The University of Manchester, Sackville Street, PO Box 88, Manchester M60 1QD, UK
[c] Unilever Research and Development, Port Sunlight Laboratory, Quarry Road East, Bebington, Wirral CH63 3JW, UK

ARTICLE INFO

Article history:
Received 3 February 2008
Received in revised form 11 July 2008
Accepted 19 July 2008
Available online 29 July 2008

Keywords:
Batch
Dispersion
Mixing
Surfactant
Silicone oil
Drop size distribution

ABSTRACT

The preparation of dilute aqueous silicone oil emulsions has been investigated with particular attention to the effect of oil viscosity (0.49–350 mPa s), impeller selection (equal diameter Sawtooth and pitched blade turbines) and the method of addition of the oil. Emulsification was found to be sensitive to how the oil was added to the vessel with narrower drop size distributions and smaller Sauter mean diameters, d_{32}, obtained when the oil was injected into the impeller region. The equilibrium values were also attained in a shorter time with the equilibrium $d_{32} \propto We^{-0.6}$. For addition of the oil to the surface the relationship was weaker with equilibrium $d_{32} \propto We^{-0.4}$. The viscosity group was particularly useful in describing the behaviour of equilibrium particle sizes for different viscosity oils and also for viscosity changes arising from different process temperatures.

An unexpected result is that the Sawtooth impellor proved to be more energetically efficient at drop break-up producing smaller droplets than the Pitched Bade Turbine. This result is particularly interesting since the power number for the latter is larger and therefore for equivalent operating conditions should produce smaller drop sizes. We suggest that one possible reason is that the local shear rates for the Sawtooth impellor are larger. Another possible reason is that the Sawtooth geometry provides more points where the local shear rates are high.

1. Introduction

It is well-accepted that local shear, elongation and necking are very important aspects of drop formation as are the physical properties of the fluids involved. Hence a successful design depends on developing a mechanistic understanding of how the equipment selection, process strategy and material properties interact to affect the resulting microstructure (e.g. particle size) and hence the performance of the products. Typically two approaches are adopted:

- Scale-up at geometric similarity and constant tip speed.
- Scale-up at equal specific power input.

Scale-up on the basis of geometric similarity and constant tip speed assumes that the relevant shear that produces the limiting drop size occurs in the agitator region where the velocity gradients are the steepest. These are assumed to scale with the peripheral velocity of the impeller and the approach generally works well if coalescence rates are low. Drawbacks of this approach are that changes in geometry require pilot scale evaluation and that if coalescence occurs then the bulk circulation time is important which, if neglected, can result in larger drops being formed on scale-up.

Scale-up at equal specific power input is generally based on the work of Kolmogorov [1] and Hinze [2] and utilises an analysis of the eddy concept of turbulence to define a limiting drop size. The theory suggests that the largest and most energetic eddies are of a size comparable to the width of an impellor blade. These are unstable and consequently break up into smaller and smaller eddies until eventually the energy is dissipated as heat by viscous flow. As energy is transferred to smaller and smaller eddies the directional nature of the flow is lost and the flow can be considered isotropic. This is known as the universal equilibrium regime consisting of two size ranges: the inertial sub-range and the viscous subrange. Eddy properties in the inertial subrange are considered solely as a function of the local energy dissipation rate per unit mass (ε_T). Eddies properties in the viscous subrange depend both on energy dissipation and viscosity.

Two mechanisms of energy dissipation are considered to contribute to drop break-up dependent on which range the prevalent

* Corresponding author. Fax: +972 9 2345982.
E-mail address: Elhamouz@yahoo.com (A. EL-Hamouz).

0255-2701/$ – see front matter © 2008 Elsevier B.V. All rights reserved.
doi:10.1016/j.cep.2008.07.008

drop break-up occurred. To determine the relevant region of break-up Kolmogorov defined an eddy length scale (η) at the boundary between the two ranges where the inertial and viscous forces are in balance and the eddy Reynolds number is equal to unity. This is equal to:

$$\eta = \left(\frac{\nu}{\varepsilon}\right)^{1/4} \tag{1}$$

where ν is the kinematic viscosity and ε is the local energy dissipation rate (W kg^{-1}).

This length scale is very much smaller than that of the primary eddies, for water at ε = 1 W kg^{-1} of η is predicted to be 32 μm from Eq. (1).

Drop diameters > η correspond to the inertial subrange and here viscous forces can be neglected. Drop diameters < η correspond to the viscous subrange where viscous forces need to be considered. Shinnar [3] claims that most drops in a stirred tank dispersion have diameters > η and are in the inertial subrange and hence the relevant stress for drop break-up is the Reynolds stress. Providing the viscosities and densities of the two phases are similar, a drop can be deformed by the flow field and may break into fragments called daughter droplets. This break-up depends on the local Weber number. Break-up occurs when the ratio $\tau(\sigma/d))$ exceeds a critical value. Shinnar [3] defined the critical drop Weber number We_{crit} for break-up in the inertial sub range as:

$$We_{crit} = \frac{\rho_c \bar{u}^2 d_{32}}{\sigma} \tag{2}$$

where $\bar{u}^2$ is the mean square of the fluctuating velocities.

The theory of Kolmogorov and Hinze assumed that drops existing in the inertial region of turbulence have a maximum size and analysis for a turbulent system shows:

$$\frac{d_{max}}{D} \propto \varepsilon_T^{-0.4} \propto We^{-0.6} \tag{3}$$

For scale up at geometric similarity a tank Weber number (We) is used. Reported values of the proportionality constant on the We expression fall in the range 0.053–0.15 [4].

Conventional dimensional analysis leads to an equation for drop size of:

$$\frac{d_{32}}{D} \propto Re^{\alpha} We^{\beta} \tag{4}$$

Experimental work has demonstrated that d_{max} is proportional to d_{32}.

For turbulent systems ($Re \geq 10^5$) α approaches zero and many (though by no means all) workers have found the exponent on β to be −0.6.

Increasing the dispersed phase viscosity leads to an increase in d_{32}/D even when the continuous phase is highly turbulent. Hinze [2] introduced a modified critical Weber number which included a viscosity group (Vi) to account for this. Other workers have built on this approach using a vessel Weber number for scale-up at geometric similarity and a modified viscosity group. For a range of silicone oil viscosities, in a range of dispersants, on three geometrically similar scales the RDT data of ref. [5] were fitted well to the following empirical equation which utilises the viscosity group:

$$\frac{d_{32}}{D} = 0.053 We^{-0.6}(1 + 0.97 Vi^{0.79})^{0.6} \tag{5}$$

where

$$We = \frac{\rho_c N^2 D^3}{\sigma}; \quad Vi = \frac{\mu_d N D}{\sigma}\left[\frac{\rho_c}{\rho_d}\right]^{0.5}$$

Vi is the viscosity group representing the ratio of dispersed phase viscosity to surface forces. The limits $Vi \to 0$ and $Vi \to \infty$ correspond to negligible viscous and surface resistance to breakage, respectively. Thus for $Vi \to 0$ Eq. (5) reduces to the expression:

$$\frac{d_{32}}{D} = C_1 We^{-0.6} \quad \text{(i.e. Eq. (3))} \tag{6}$$

Calabrese et al. [6] shows then when $Vi \to \infty$, the theoretical expression that yields the form of Eq. (5) reduces, for geometrically similar systems, to the form of:

$$d_{max} = C_2(\rho_c \rho_d)^{-3/8} \mu_d^{3/4} \varepsilon_T^{-1/4} \quad \text{or} \quad d_{32} = C_3(\rho_c \rho_d)^{-3/8} \mu_d^{3/4} \varepsilon_T^{-1/4} \tag{7}$$

The counterpart of Eq. (5) has been expressed in dimensionless form containing a Reynolds number. It was pointed out by ref. [6] that this is misleading as the continuous phase viscosity term cancels.

The Sauter mean diameter, d_{32}, is commonly used to characterise the size distribution because it is inversely proportional to the total surface area of the dispersed phase and thus particularly useful when considering to mass transfer and chemical reactions [4]. A mathematical definition of d_{32} is the ratio of the third and the second density function of droplet diameters.

$$d_{32} = \frac{\int_{d_{min}}^{d_{max}} d^3 p(d) \Delta d}{\int_{d_{min}}^{d_{max}} d^2 p(d) \Delta d} \tag{8}$$

where d is the particle size and $p(d)$ is the proportion of material with that size. The integral limits d_{min} and d_{max} are respectively the minimum and maximum drop sizes.

To a process engineer the ideas of Kologoroff and Hinze are attractive. If break-up is due to turbulent shear and takes place in regions of isotropic turbulence then energy and flow alone dictate agitator type and geometry. One of the implications, which we investigate here, is that the addition point should not matter providing the agitator is operated above the dispersion speed and the mixing time is much shorter than the processing time. Nienow [7] wrote that "processes which are particularity dependent on turbulent eddies and their associated forces are likely to be well correlated by energy dissipation rate. Gas–liquid mass transfer rates, liquid–liquid drop sizes and gas–liquid hold-up fall into that category".

There are many reported anomalies. For example, refs. [8,9] reported that drop size decreases on scale-up at constant power per unit mass. Also different agitator types have been reported to produce different drop sizes in the same vessel at the same power per unit mass [10]. Some exponents of the theory argue that the anomalies are due to applying a tank mean ε_T whereas most of the break-up occurs in the agitator region. As a consequence, it would be more appropriate to use the agitator (or even individual blade) swept volumes in the power per unit mass estimates. The reduction in drop size on scale up applying turbulence theory can be explained by intermittency, for example, refs. [11,12,35].

Prediction of the drop size distribution in turbulent dispersions using the theories of Hinze–Kolmogorov has been the subject of a considerable body of experimental and theoretical studies [e.g. 13–22]. The effect of dispersed phase viscosity on drop break-up was studied extensively by ref. [6] where they correlate d_{32} to both We and viscosity numbers. Most of the work published in the literature (except refs. [6,12,13]) is for a low viscosity dispersed phase and surfactant-free systems. This is clearly shown in Table 1, where only

Table 1
Published work related to liquid–liquid dispersion with respect to dispersed phase viscosity and surfactant use

Investigators	System used					
	Concentration	ρ_c (kg m^{-3})	ρ_d (kg m^{-3})	μ_d (mPa s)	Volume, V (L)	Interfacial tension, σ (mN m^{-1})
[4]	0.01–0.3 toluene heavy oil water	998	895	1.56	0.91	19.9
[5]	Silicone oil–aqueous methanol water	997–792	834–968	1–1000	2.65	1 for 100% methanol 45 for 0% methanol
[6]	Silicone oil–water	997	960–975	100–10,000	2.2–50	37.8
[10]	0.03% silicone oil water	998	1050	173.2	10.8	45
[11]	0.3% silicone oil water	1000	900–975	10–1000	2.65	45–50
[12]	0.0038 silicone oil in double ionized water	998	1050	10–1000	2.6	45–50
[13]	0.1% *n*-dodecane–water	1000	850	1	0.5	72.2
[14]	0.01–0.1 kerosene–water	1000	794	0.93	21.5	38.7
[23]	0.02% styrene–water 0.02 octanol–water	–	823 900	0.72 7.49	2.8	34 (no surfactant), 8.3 with surfactant
[24]	Mixture of silicone oil in glycerol–water mixture	–	–	Mixture of 20 and 350	0.8	12.6–18.8, 0.3% Tween surfactant
[27]	1–5% chlorobenzene–water 1–5% sunflower oil–water	1000 1000	1106 919	0.75 55	2.65, 1.5	33.4 27
[34]	0.0078 hydroxyoxime	1021	815	1–2	12.7	Not mentioned
[35]	1% chlorobenzene–water	1000	1016	1	2.65, 21.5	33.4
[36]	Benzene–CCL4/water Heptane–CCL4/water Acetophenone/water Dimethylpolysiloxane CCL/water	– – – –	– – – –	0.74 0.72 1.6 11.3	1.7	35 42 17.4 36.2
[37,38]	1% styrene–water with PVA	997 988	901 879	0.73 0.459	2	11.5 (25 °C) 7.4 (50 °C)

refs. [23,24] investigated the effect of surfactant on drop breakage in turbulent liquid dispersion of low viscosity.

2. Experimental

The main aim of this work was to examine the mechanisms involved in the emulsification of silicone oils in an industry standard batch mixer (ESCO EL6 from ESCO-Labor AG). In subsequent work we intend to work at larger scale so that we can determine the scale-up parameter. The mixer used in this study is a 6 L R&D unit typically used by the health care industry for prototyping structured liquid products such as toothpaste, shampoo or hair conditioner. This mixer consists of a scraped wall anchor for bulk mixing and a high speed, high shear mixer for drop size reduction and dispersion. The size reduction and dispersion steps are critical to the final product quality and important design considerations are:

- What type of disperser should we use?
- What is the effect of the position where we add the oil?
- What is the effect of agitation rate on the dispersion?
- How does the energy dissipation rate effect the dispersion?
- How do we scale-up or down to produce the same drop-size distribution between similar/dissimilar equipment?

To deliver these aims, a programme of work was developed to measure the drop size distribution of silicone oil–water dispersions in presence of sodium laureth sulphate (SLES) surfactant under different mixing conditions using two types of impellers (Sawtooth and PBT) and a range of impeller speeds, dispersed phase viscosity and addition position.

2.1. Equipment

Experiments were carried out in a standard ESCO mixer (ESCO-Labor AG) shown in Fig. 1. The vessel has a working volume of 6 litres with a 20 cm internal diameter with a standard geometry scraped wall anchor blade inside (this can viewed in Figs. 1 and 2). In addition a high shear impeller can be fitted to one side of the main shaft and can be operated in conjunction with the anchor or by itself. Two high shear impellers were examined in this study namely a 5 cm diameter Sawtooth impeller (shown in Fig. 2) or a 5 cm diameter down pumping 45° four pitched blade turbines (PBT). The power numbers of both impellers were measured at turbulent Reynolds numbers using a calibrated torque strain gauge connected to an ASTECH telemetry system. The measured power numbers were 0.32 for the Sawtooth and 0.99 for the PBT.

2.2. Materials

The model system is an oil-in-water emulsion where the oil phase is silicone oil (Dow corning oil 200 fluid). Various grades of oil were used with viscosities varying from 0.49 mPa s to 350 mPa s. The surfactant stabiliser is SLES which is a mixed alkyl ether sulphate (C_{12-14}) with EO sodium salt. The grade used is a commercial sample (from Cognis UK Ltd., Hertfordshire, UK) and comes as a viscous yellow liquid of specific gravity of 1.03–1.04. SLES is a widely used in many household and personal care products because it is a good stabiliser for a wide range of oils. Our choice of a commercial grade of SLES rather than a purified analytical grade is because in subsequent work we would like at much larger scales where the cost of purchasing sufficient pure surfactant would be prohibitive.

Our principle interest is in systems where only break-up occurs and coalescence is absent. Also when considering the trials where

Fig. 1. ESCO 6 L mixer.

the oil was added into the impeller region we wanted to keep the addition time short. Consequently we chose to work at low phase volumes (1% silicone oil) and with surfactant concentration well above the CMC. In addition operating with dilute emulsions had the added advantage that flow visualization was possible and viscosity could be assumed to be that of water alone.

2.3. Experimental procedure

The ranges of parameters used in the experiments are listed in Table 2 and the experimental procedure was as follows.

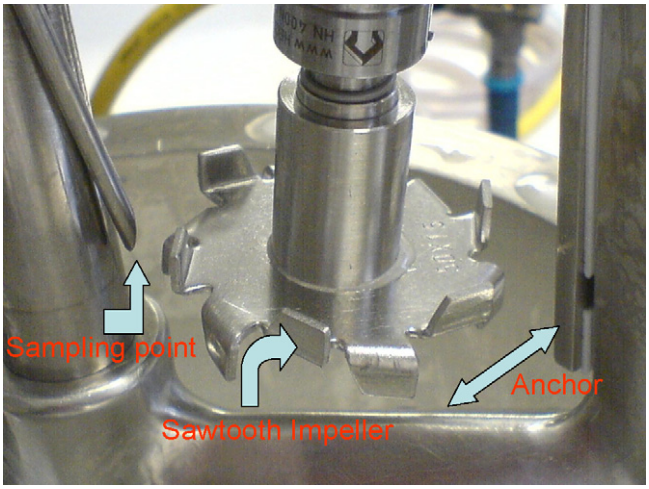

Fig. 2. Sawtooth impeller and the sampling point.

Table 2
Experimental parameters used

Parameter	Value
Dispersed oil viscosity (mPa s)	0.49, 18.9, 48 and 339
Impeller type	High shear Sawtooth and PBT
Impeller diameter	0.05 m
Impeller speed (rpm)	1100, 2000 and 3000
Injection position	Surface and impeller
Reynolds number	38,250 to 186,000
Operating temperature (°C)	25, 40
SLES concentration (ppm)	7090

1 The surfactant solution was prepared by charging the vessel with deionised water and then the required amount of SLES. The solution was then heated by the jacket to the required temperature while the contents were continuously stirred by the anchor. An anchor speed of 50 rpm was selected to help mix the surfactant solution and ensure a well mixed and thermally uniform solution but without causing any aeration of the solution. Once the required temperature was reached mixing was continued for another 5 min and then the anchor was switched off.
2 In the experiments where the oil was added to the surface an amount equivalent to 1% (w/w) of the silicone fluid was carefully and slowly poured onto the surface of the water phase with the aid of the conical funnel shown in Fig. 1. Once this was completed high speed stirrer was switched on and the timer started. In the case of impeller addition, the oil was injected over a period of 20 s into the impellor region using a syringe. The timer was started as soon as all the oil had been added.
3 A sample of 20 ml of the suspension was taken through the sampling point. The sampling point was set at 1 cm from the outside of the high shear impeller at the level of the impeller, as shown in Fig. 2. Samples were aspirated using a syringe attached to a Teflon capillary. The sample was then taken to the Malvern Mastersizer 2000 to measure the drop size distribution. It was found that samples measured directly after withdrawal gave the same results as samples measured after one day. In fact no significant difference in the distribution was noted even after a month providing the sample was well mixed before analysis. This stability was a result of the presence of the SLES surfactant. Sampling was repeated at fixed time intervals until the measured Sauter mean diameter did not change with time. Sampling was carried out after 3, 8, 15, 25, 35, 45 and 60 min and then after 2, 4, 6 h and finally after 24 h. The experimental data were fitted to a first order exponential from which the equilibrium d_{32} was found.

The impeller speed ranges were chosen so that the lowest impeller speed gives a Reynolds number above 20,000 (fully turbulent region) and is above the minimum dispersion speed. In the trials we wanted to avoid surface aeration and so we used a clear Perspex vessel of the same specification as the ESCO mixing vessel to make visual observations at various impeller speeds. In this way we were able to set a maximum impeller speed.

All experiments were carried out at a temperature of either 25 °C or 40 °C. Due to the flammability value of the 0.49 mPa s oil, experiments involving this oil were carried out only at 25 °C. Oil viscosities and oil water interfacial tension in the presence of SLES were measured at these two temperatures. SLES (0.5% by weight) was dissolved in deionised water, which is nine times the SLES CMC value. Very recently, the effect of the SLES concentration on the mean drop size even up to concentrations 84 times the measured CMC was measured by ref. [25]. It was found that excess amount of SLES concentration above the CMC value still has an effect on the drop size distribution. This effect was related to the increase of the interfacial area at the oil–water interface with time and also

Table 3
Physical properties of Dow corning oil

Measured viscosity of Dow corning oil at different temperatures (mPa s)		Measured interfacial tension (mN m^{-1})		Refractive index at 25 °C	Density at 25 °C (kg m^{-3})
25 °C	40 °C	25 °C	40 °C		
0.49	–	13	11.60	1.375	759
18.9	12.3	13.2	11.69	1.40	946
48	32.2	13.2	11.69	1.401	957
340	242	13.1	11.71	1.403	967

with depletion of surfactant in the bulk. Two different slopes of the change of the droplet median with time were found as a result. A Haake RV20 viscometer fitted with a MV2 rotor was used for measuring the viscosity and a Kruss drop volume tensiometer, Model DVT-10, was used for the interfacial tension measurements. Results are shown in Table 3.

Particle size measurements were made on a Malvern Mastersizer 2000 equipped with Hydro SM small volume sample dispersion unit. The Malvern measured particles in a size range of 0.02–2000 μm with an accuracy of ±1% on volume median diameter. The data was analysed using a polydisperse model with the dispersed phase density set at 0.97 g cm^{-3} except for the 0.49 mPa s oil which had a significantly lower density of 0.76 g cm^{-3}. The presentation used the measured refractive index (RI) of the dispersant of 1.33 and the oil the oil of 1.451. The imaginary part was set to zero. The measurement technique is well known and is not described in detail here. The calibration of the instrument was, however, checked using standard particles before each experiment. The same sampling and measurement method was used successfully by refs. [4] and [13].

3. Results

3.1. Effect of dispersed phase viscosity

Fig. 3 presents a set of experiments using the Sawtooth impeller (3000 rpm) and carried out at 40 °C with various oils placed on the surface of the aqueous phase. The figure shows that higher viscosity oils produce larger equilibrium Sauter mean diameter ranging from 25 μm for the 242 mPa s oil to about 6.5 μm with the 0.49 mPa s oil. Also, lower dispersed oil viscosity approaches the equilibrium d_{32} value faster than the more viscous oil. Experimental data (shown in the figure as points) were fitted to an exponential first order equation. This is shown in the figure as solid lines. The lowest regression value of the fitting was 0.93. This method gave an indication of the approach to the equilibrium d_{32} and allows estimating the equilibrium value. The calculated equilibrium value of d_{32} by the first

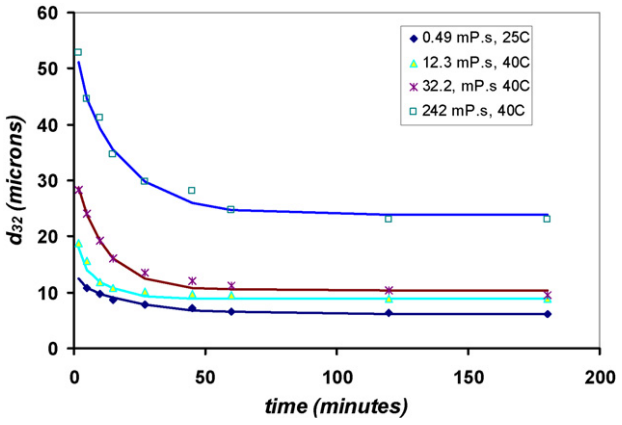

Fig. 3. Sauter mean diameter of different silicone oils at 3000 rpm.

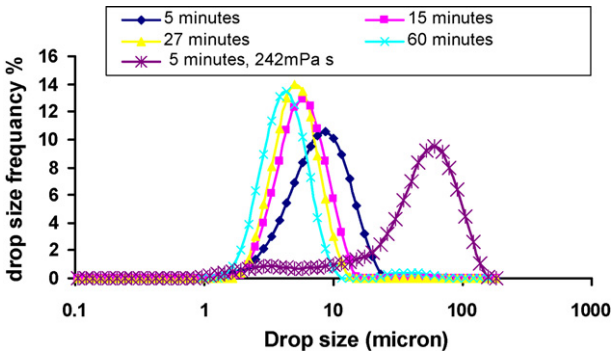

Fig. 4. Evolution of the drop size distribution with time for 0.49 mPa s silicone oil using Sawtooth impeller at 3000 rpm.

order fitting is ±3% of the measured value of d_{32} after 24 h. This is evident as the lines approach its asymptotic value. The goodness of 'fit' to a first order equation confirms that the process is primarily that of the drop break-up. The use of surfactant SLES and the low oil phase volume effectively eliminates coalescence.

The evolution of the drop size distribution with time for the 0.49 mPa s silicone oil is depicted in Fig. 4. The mean diameter of the dispersed oil reduces with time and the distribution width becomes narrower. This is evident from the decrease of the span of the distribution with time. Span is a measurement of the width of the distribution and is represented here mathematically by,

$$\text{span} = \frac{d_{0.9} - d_{0.1}}{d_{0.5}}$$

The Malvern output contains the $d_{0.1}$, $d_{0.5}$ and $d_{0.9}$ data. In Fig. 4, at 5 min the span is 1.34, decreasing to 1.08 at 15 min and 0.99 at 60 min. A drop size distribution for the 242 mPa s at 5 min is shown for illustration at the same figure. For the 242 mPa s oil, the span changes from 1.85 at 5 min to 1.6 after 60 min. Span values of other oils of intermediate viscosity change qualitatively in similar way with the span at any time point increasing with viscosity are shown in Table 4.

3.2. Impeller type and speed

A comparison of emulsification of the 242 mPa s viscous oil by the Sawtooth and PBT impellers is shown in Fig. 5. The two impellers are of equal diameter although the power number for the latter is higher. Consequently for identical rotor speeds the power consumption and hence the mean energy density of the higher *Po*

Table 4
Span values for silicone oil of different viscosities

Time (min)	Span value			
	0.49 mPa s	12.3	32.2	242 mPa s
5	1.34	1.46	1.62	1.85
15	1.08	1.36	1.57	1.75
60	0.99	1.14	1.50	1.60

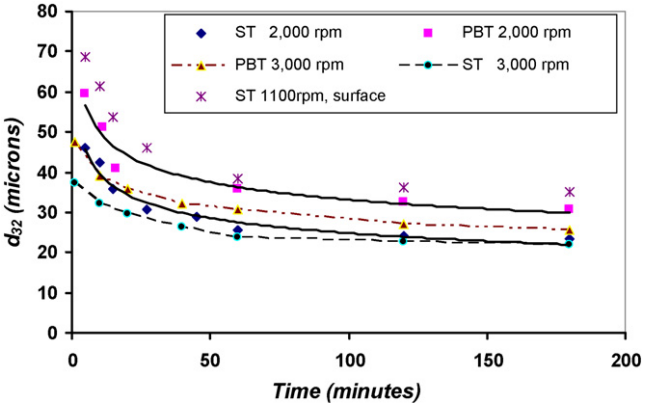

Fig. 5. Comparison between Sauter mean diameter of Sawtooth (ST) and PBT at 2000 and 3000 rpm.

impeller would be higher and therefore the particle size would be smaller. However, contrary to our expectation it is clear from Fig. 5 that the smaller droplets are produced by the impeller with the lower *Po* (i.e. the Sawtooth impeller). In addition the span of the size distribution for the Sawtooth is smaller than that of the PBT.

In the case of the PBT at 2000 rpm, it is not clear if the equilibrium d_{32} value has been reached. Wang and Calabrese [5] discus the equilibrium transient drop sizes in turbulent flow and report that several hours are required for a dilute dispersion to achieve equilibrium. The equilibrium time increases on scale-up. Leng and Calabrese [26] discuss this phenomena and note that the long time behaviour ($t \rightarrow \infty$) is uncertain. Some workers argue that d_{32} decreases without limit whilst other workers found that actually d_{32} increases at long time. Using an analogy to reaction kinetics some researchers have suggested that the break-up can be described by a kinetics type equation containing a rate constant and an order term. For first order behaviour d_{32} reduces exponentially with time. Our data appears to fit an exponential decay model fairly well and we have used this type of expression to estimate the equilibrium value by fitting the experimental data to a first order regression (solid lines) to extract the equilibrium d_{32} value. The equilibrium values obtained by this process are used in the subsequent correlations presented here.

These findings clearly indicate that the selection of impellers for emulsification is not straightforward and that there can be processing advantages from choosing a low power number impeller when small drops of a narrow size distribution are required. This surprising result may indicate that local shear, rather than turbulent shear is the chief architect of drop breakage. Certainly ε_T is not sufficient to predict d_{32}. Pacek et al. [27] also found that the low power number agitators produced smaller drop sizes at equal impeller diameter and energy dissipation rates. They argued that this was due to the lower power number impeller having a shorter circulation time, so that the drop goes through the impeller region more frequently. However, in this present case the comparisons are done at the same agitation speed and impeller diameter. Because of the absence of radial vanes on the Sawtooth blade the pumping rate is much lower than a conventional impeller. Beck [28] measured a flow number of 0.043 for an EKATO mizer-disk (a specialist Sawtooth disperser) which is an order of magnitude less than a pitch blade turbine so we would expect the circulation times for the Sawtooth to be in fact much longer. One major difference is that the Sawtooth impeller has many more shearing points than the PBT. Beck [28] found that, compared at equal diameter and specific power, the EKATO mizer-disk produced much smaller drops than a Rushton turbine (a factor of 3–4 times smaller) [28].

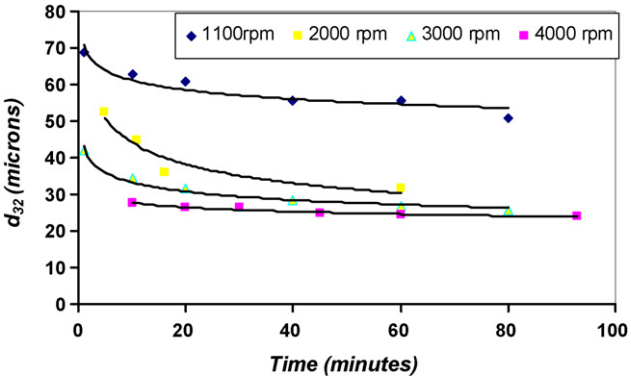

Fig. 6. Variation of Sauter mean diameter with speed using PBT impeller for the 242 mPa s silicone oil.

Fig. 6 presents the evolution of the mean particle size for increasing rotor speed of the PBT. We again see that as the rotor speed increased the drop size decreases. At 4000 rpm (higher shear and energy dissipation) the Sauter mean diameter is a fairly flat function of process time with an equilibrium particle size of about 24 μm. With power consumption proportional to N^3 and the pumping rate proportional to ND^3 then a doubling of the speed results in eight times the energy dissipation and a doubling of the frequency with which drops pass through the impeller zone. This may explain the nearly horizontal shape of the Sauter mean diameter with time at 4000 rpm. At 3000 rpm equilibrium is achieved after about 60 min but at low impeller speed (1100 rpm) d_{32} value is still decreasing and equilibrium has not been reached.

It is necessary to stress that at 4000 rpm, there was slight surface aeration. However, when the impeller was stopped; the air bubbles disappeared in a very short time and therefore would not be expected to affect the drop size measurements.

3.3. Addition of oil into impeller region

To investigate the effect of addition point of the dispersed phase, a further set of experiments were carried out with the Sawtooth impeller at 40 °C but with the oil added close to the impeller at (1 cm from the impellor but on the impeller centreline). Fig. 7 presents the data for the viscous oil (242 mPa s) but similar results were obtained for the thinner oil (32.2 mPa s). The initial breakage of the drops was faster in comparison to the breakage when oil was injected at the top surface. This is more pronounced in the case of 1100 rpm (which is shown in Fig. 5) as the Sauter mean diameter changes from 71 μm at 3.5 min to 37 μm after 1 h and reaches its equilibrium value after

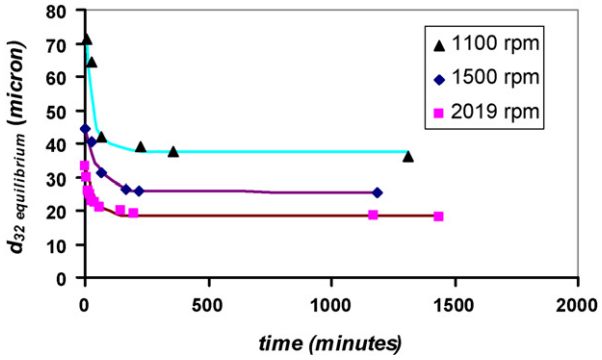

Fig. 7. Sauter mean diameter for the Sawtooth impeller as a function of speed for 242 mPa s silicone oil added to the impeller region.

3 h. Results shown in Fig. 7 were reported for more than 16 h in order to make sure about the time to reach equilibrium.

The same experiments were repeated using 32.2 mPa s oil and similar qualitative behaviour was observed. Also it was found that the lower dispersed oil viscosity approaches the equilibrium value faster than the more viscous oil.

4. Discussion

4.1. Viscosity number

Substituting the values for the material properties in Table 3 along with typical rotor speeds yields values of *Vi* varies from 2 to 60. Equilibrium drop sizes for both the Sawtooth and PBT for various rotor speeds and viscosities are presented in Fig. 8 as a function of the viscosity number. The figure shows that as the viscosity number decreases the equilibrium drop size also decreases. More importantly the figure shows that the viscosity number is the appropriate dimensionless grouping to describe the effects of rotor speed and oil viscosity.

The data presented in Fig. 8 are best correlated by

$$d_{32} = 4.47Vi^{0.46} \quad (9)$$

with a regression coefficient R^2 of 0.98. From the definition of the viscosity group, *Vi* this correlation cannot be valid for very small value of viscosity group ($Vi \ll 1$) as the effect of interfacial tension will be much higher than the effect of the dispersed phase viscosity.

4.2. Weber number

A plot of the equilibrium d_{32} rendered dimensionless by the impeller diameter as a function of Weber number is shown in Fig. 9. On the same figure, results for two different viscosities and also a comparison of surface and impeller addition of the oil are included. The following correlations were found for the 242 and 32.2 mPa s oils (Eqs. (10) and (11), respectively) with a regression R^2 value over 0.99 for the two correlations

$$\frac{d_{32}}{D} = 0.187We^{-0.60} \quad (10)$$

$$\frac{d_{32}}{D} = 0.183We^{-0.64} \quad (11)$$

From theory (recall Eq. (3)) the value of the exponent on *We* is −0.6 and our experimentally determined values are in close agreement with this theoretical value. However the equivalent correlation for the more viscous 242 mPa s oil added to the surface of the aqueous phase has a much lower exponent, −0.41. This value is consistent with the values obtained by ref. [17] who obtained values of between −0.43 and −1 using various impeller types. However the deviation of the exponent from −0.6 does not mean that coalescence is the dominant process. This was tested by obtaining the equilibrium d_{32} for an impeller speed of 2000 rpm followed which the impeller speed was reduced to 1100 rpm and measuring the new equilibrium d_{32}. There was no significant difference between the two equilibrium values (19.5 μm for 2000 rpm and 20 μm at 1100 rpm).

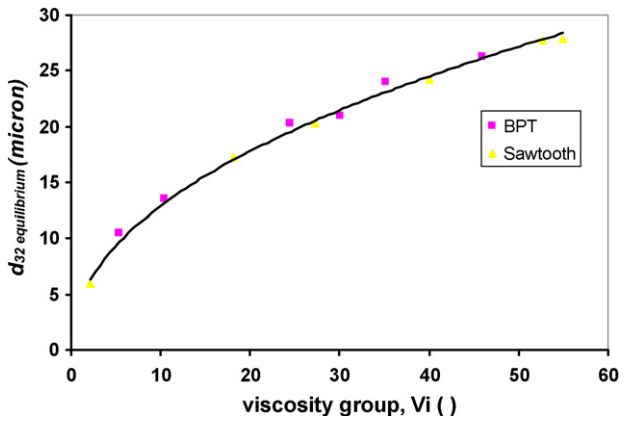

Fig. 8. Equilibrium Sauter mean diameter as a function of viscosity group for both the Sawtooth and PBT impellers.

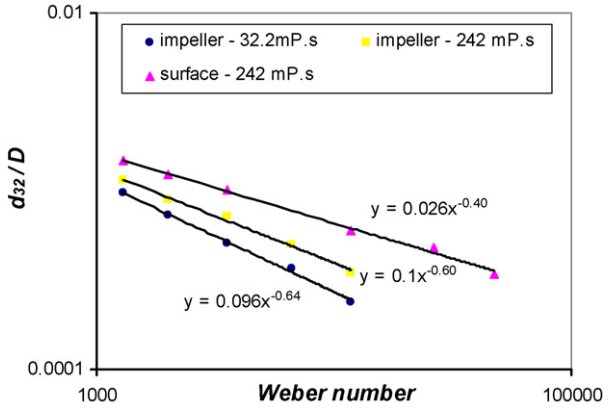

Fig. 9. Equilibrium Sauter mean diameter using Sawtooth impeller as a function of Weber number at two addition positions and two oil viscosities.

Our findings therefore show that the breakage process of silicone oil added to the surface is slower than that of addition into the impeller region. When the process is observed in Perspex vessel rather than in the ESCO vessel we see some clear differences in behaviour (Fig. 10). In the case where the oil is added to the surface of the aqueous surfactant solution (a–c) we see that as the oil is drawn down long filaments are formed which break off into large primary drops. Buoyancy then tends to keep these drops close to the surface and it can take some time for them to be drawn down into the impeller region. When these large drops are eventually captured by the impeller, they are broken into smaller drops which are then dispersed through the tank. Experiments have also shown that the maximum drop size did not change very much during long agitation time. This suggests strongly asymmetric breakage (stripping of very small daughter drops from the mother) which means that erosion is most probably the predominant type of breakage. Note that with the high level of SLES, coalescence is effectively suppressed. On the other hand Fig. 10(d)–(f) shows how quickly silicone drops were broken when injected into the impeller region. A large number of very small drops are created in a shorter time compared to the surface addition. This is because drop breakage takes place primarily in the impeller zones, so drop sizes do not change in the bulk. Flow visualisation confirmed that all the break-up (either of the large mother drops in the case of surface injection, or the material added directly into the impeller region) was confined to a region very close to the agitator blades as found by many other workers.

4.3. Mean energy dissipation rate and tip speed

There is a continuing debate on whether the energy dissipation rate (mean or maximum) or the tip speed should be used for scale up. For the flow in agitated tank, reported values of the ratio of intense turbulent energy dissipation rate ε_{max} to a tank average turbulent energy dissipation rate ε_T vary. The mean turbulent energy is obtained from the classical expression of agitator power = $Po\ \rho N^3 D^5$ by dividing this by the total mass of fluid. Where *Po* is the impeller

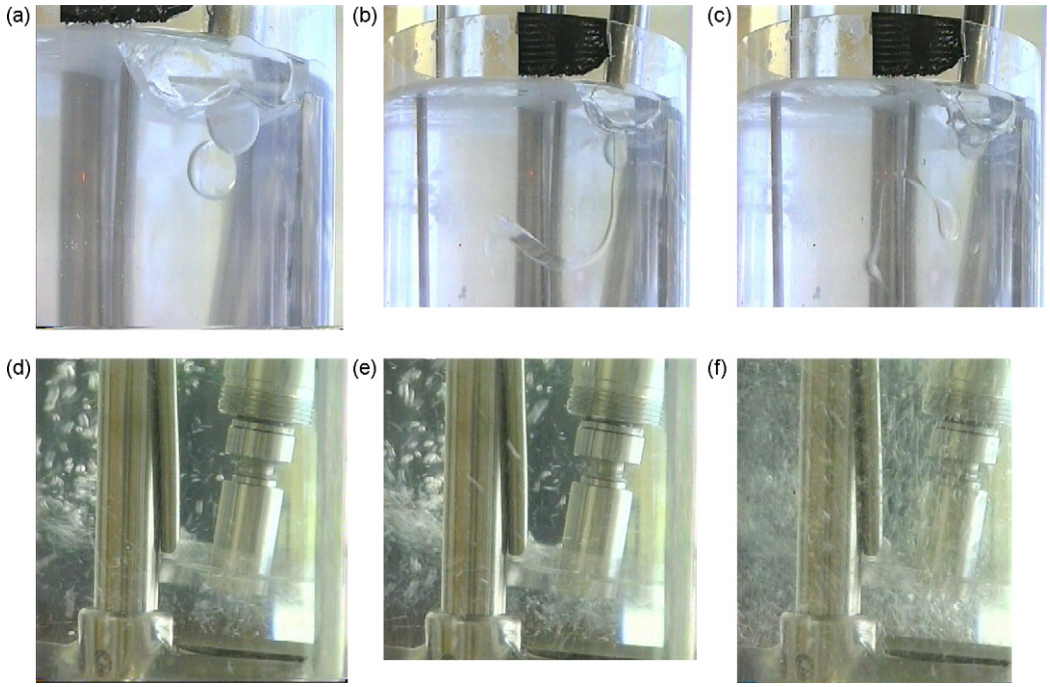

Fig. 10. Drop deformation and resulting daughter drops of silicone oil at 2000 rpm. Parts (a)–(c) are for surface addition and (d)–(f) are impeller addition.

power number, D is the impeller diameter, N is the impeller speed (in rps), and ρ is the continuous phase density (kg m^{-3}). The highest ratio of $\varepsilon_{max}/\varepsilon_T$ reported by ref. [29] was 270 but most reported values are smaller than 100 [30–33].

Fig. 11 presents the equilibrium particle size as a function of the mean energy dissipation rate and shows that the lower *Po* impeller (namely the Sawtooth) produces smaller droplets for the same energy dissipation rate. Interestingly the indices on ε_T of −0.24 is very close to the value of −0.25 predicted from turbulence theory (Eq. (7)) for viscous drops. It is however clear that mean turbulent energy dissipation rate ε_T is not always sufficient to describe the breakup performance across different impellers. As a consequence the idea of a maximum turbulent energy dissipation rate (ε_{max}) per unit mass has been introduced to account for such differences. The reasoning is as follows. Drop break-up predominantly occurs in the highest shear or strongest turbulence energy dissipation region. Typically these will be close to the impeller where we might reasonably expect the turbulence to be non-isotropic and therefore agitator and geometry dependent. Only a small proportion of the turbulent energy dissipation occurs in the bulk of the vessel where isotropic turbulence exists. A value of ε_{max} is usually taken to be 100 times ε_T, however, to be of more general use across impeller types the actual volume over which the energy is dissipated must be determined. However this is impeller specific and there is a still a big question of how easily and accurately one can measure ε_{max}. Zhou and Kresta [10], further argue that as well as the maximum energy dissipation rate, the circulation time should also be used.

An alternative scale up criteria for emulsification is the tip speed ($\propto(ND)$). For the present work, d_{32} can be correlated to the tip speed to yield the following correlations for the PBT and Sawtooth, respectively.

$$d_{32} = 50.1(ND)^{-0.73} \quad (12)$$

$$d_{32} = 46.0(ND)^{-0.73} \quad (13)$$

Both correlations result in a R^2 regression value of more than 0.98. The two correlations are very similar so in Fig. 12 only a single correlation is presented to the combined data set from the two impellers (regression value of 0.97).

$$d_{32} = 48.0(ND)^{-0.73} \quad (14)$$

For the purpose of scale up consideration, it is planned to repeat the experiments at geometrically similar scale in order to inves-

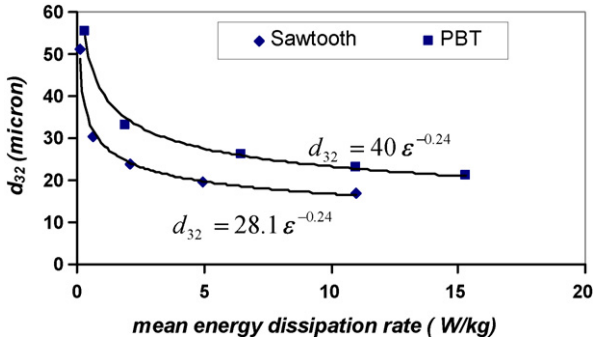

Fig. 11. Regression of d_{32} equilibrium as a function of mean energy dissipation rate.

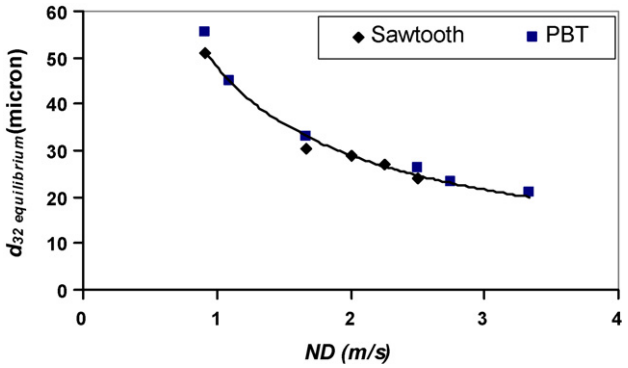

Fig. 12. Equilibrium Sauter mean diameter as a function of tip speed for both Sawtooth and PBT impellers.

tigate the scale up rules. Therefore, a tip speed and mean energy dissipation rate will be investigated.

5. Conclusions

Drop size distribution of silicone oil-in-water emulsions in the present of surfactant solution are presented for Sawtooth and PBT impellers, for various impeller speeds, oil viscosities and two addition points for the oil phase.

- Our results indicate that rotor tip speed is a better means of predicting particle size than mean energy dissipation rate. By comparing the emulsification performance of two different but equal diameter impellers we were able to show that, contrary to our expectation, for equivalent speeds the low power number impeller (and hence lower mean energy dissipation rate) produced the finer droplets. It should be noted however that turbulent kinetic energy is proportional to tip speed and hence we cannot dismiss turbulence theory. Also we found a dependence of d_{32} to ${\varepsilon_T}^{-0.24}$ close to the dependence of ${\varepsilon_T}^{-0.25}$ predicted from turbulence theory for viscous drops in two phase dispersions. In addition the dimensionless viscosity number is an effective way of describing the effect of variation in dispersed phase viscosity.
- We further conclude that the point at which the oil is added to the tank is crucial in achieving a small and uniform particle size. Adding the dispersed phase directly into the impeller region (as opposed to the surface) produced smaller drops of a narrower size distribution and the equilibrium d_{32} was achieved in shorter time. Correlations with *We* revealed that for oil addition into the impeller region followed the classical relationship with an exponent of −0.6. However when the oil was added to the surface the relationship to We was much weaker with an exponent of −0.4.
- Flow visualization showed very different behaviour between the two modes of oil addition. When the oil is added to the surface emulsification occurred in two stages. Firstly the formation of very large droplets close to the surface as the impeller tries to draw down the oil. The natural buoyancy of the oil resists this tendency and the large droplets can remain close to the surface for some time. Secondly when the oil is eventually drawn into the impeller region and passes through it they were broken into a number of daughter drops. On the other hand adding the oil directly into the impeller region only the second stage is observed. We conclude that the draw down of the oil and/or very large drops is the limiting factor and is responsible for the lower than expected exponent on *We* observed.

Acknowledgments

The authors would like to thank Mr. John Yoke from Unilever Research and Development (URD) for his assistance in measuring the interfacial tension. Thanks are also due to An-Najah National University for the sabbatical leave granted to Dr. El-Hamouz.

Appendix A. Nomenclature

d_{32}	Sauter mean diameter (m)
D	impeller diameter (m)
D_{max}	maximum stable drop size (m)
N	impeller speed (s^{-1})
ND	proportional to tip speed ($m\,s^{-1}$)
$p(d)$	proportion of material with size d
Po	impeller power number
Re	Reynolds number
T	tank diameter (m)
Vi	viscosity number
We	Weber number

Greek letters

α	exponent on Reynolds number
β	exponent on Weber number
ε_{max}	maximum energy dissipation rate per unit mass (m^2/s^3)
ε_T	mean energy dissipation rate in the tank per unit mass (m^2/s^3)
η	Kolmogorov's length scale (m)
μ_d	dispersed phase viscosity (Pa s)
ρ	Density ($kg\,m^{-3}$)
σ	interfacial tension (Pa s)

Subscripts

c	refers to the continuous phase
d	refers to the dispersed phase

References

[1] A.M. Kolmogorov, Breakup of droplets in turbulent flow, Dokaldy Akademii Nauk Uzbekskoi SSR 66 (1949) 825–828.
[2] J.O. Hinze, Fundamentals of the hydrodynamic mechanism of splitting dispersion process, AIChE J. 1 (1955) 289–295.
[3] R. Shinnar, On the behaviour of liquid dispersions in mixing vessels, J. Fluid Mech. 10 (1961) 259–275.
[4] C.W. Angle, H.A. Hamza, Predicting the sizes of Toluene-diluted heavy oil emulsions in turbulent flow: Part 2: Hinze-Kolmogorov based model adapted for increased oil fractions and energy dissipation in a stirred tank, Chem. Eng. Sci. 61 (2006) 7325–7335.
[5] C.Y. Wang, R.V. Calabrese, Drop breakup in turbulent stirred-tank contactors: Part II: Relative influence of viscosity and interfacial tension, AIChE J. 32 (4) (1986) 667–676.
[6] R.V. Calabrese, T.K.P. Chang, P.T. Dang, Drop breakup in turbulent stirred contactors: Part 1: Effect of dispersed phase viscosity, AIChE J. 32 (4) (1986) 657–666.
[7] A.W. Nienow, Hydrodynamics of stirred bioreactors, Appl. Mech. Rev. 51 (1998) 3–32.
[8] G.W. Colenbrander, Experimental findings on the scale-up behaviour of the drop size distribution of liquid/liquid dispersions in stirred vessels, in: Proceedings of the 10th European Conference on Mixing, Delft, Netherlands, 2000, pp. 173–180.
[9] M. Musgrove, S. Ruszkowski, Influence of impeller type and agitation conditions on the drop size of immiscible liquid dispersion, in: Proceedings of the 10th European Conference on Mixing, Delft, Netherlands, July 2–5, 2000, pp. 165–172.
[10] G. Zhou, S.M. Kresta, Correlation of mean drop Size and minimum drop size with the turbulence energy dissipation and the flow in an agitated tank, Chem. Eng. Sci. 53 (11) (1998) 2063–2079.
[11] W. Podgorska, J. Baldyga, Scale-up effects on the drop size distribution of liquid-liquid dispersions in agitated vessels, Chem. Eng. Sci. 56 (3) (2001) 741–746.
[12] W. Podgorska, Modelling of high viscosity oil drop breakage process in intermittent turbulent, Chem. Eng. Sci. 61 (2006) 2986–2993.
[13] H. Sis, G. Kelbaliyev, S. Chander, Kinetics of drop breakage in stirred vessel under turbulent conditions, J. Dispersion Sci. Technol. 26 (2005) 565–573.
[14] D. Sechremeli, A. Stampouli, M. Stamatoudis, Comparison of mean drop sizes and drop size distribution in agitated liquid-liquid dispersions produced by disk an open type Impellers, Chem. Eng. J. 117 (2006) 117–121.
[15] J. Alvarez, J. Alvarez, M. Rendez, A population approach for the description of particle size distribution in suspension polymerization reactors, Chem. Eng. Sci. 49 (1994) 99–113.
[16] G. Zhou, S.M. Kresta, Evolution of drop size distribution in liquid-liquid dispersions for various impellers, Chem. Eng. Sci. 53 (11) (1998) 2099–2113.
[17] A.W. Pacek, C.C. Man, A.W. Nienow, On the Sauter mean diameter and size distributions in turbulent liquid/liquid dispersions in a stirred vessel, Chem. Eng. Sci. 53 (11) (1998) 2005–2011.
[18] J.C. Lasheras, C. Eastwood, C. Martinez-Bazan, J.L. Montanes, A review of statistical models for the break-up of an immiscible fluid immersed into fully turbulent flow, Int. J. Multiphase Flow 28 (2002) 247–278.
[19] S. Ceylan, G. Kelbaliyev, K. Ceylan, Estimation of the maximum stable drop sizes, coalescence frequencies and the size distribution in isotropic turbulent dispersions, Colloids Surf. A Physicochem. Eng. Asp. 212 (2003) 285–295.
[20] J.B. Fernandes, M.M. Sharma, Effective interfacial area in agitated liquid-liquid contactors, Chem. Eng. Sci. 22 (1967) 1267–1282.
[21] D.E. Brown, K. Pitt, Effect of impeller geometry on drop break-up in a stirred liquid-liquid contactor, Chem. Eng. Sci. 29 (1974) 345–348.
[22] D. Daglas, M. Stamatoudis, Effect of impeller vertical position on drop sizes in agitated dispersions, Chem. Eng. Tech. 23 (2000) 437–440.

[23] A. Koshy, T.T. Das, R. Kumar, Effect of surfactants on drop breakage in turbulent liquid dispersions, Chem. Eng. Sci. 43 (3) (1988) 649–654.
[24] S. Kumar, V. Ganvir, C. Satyanand, R. Kumar, Alternative mechanism of drop breakup in stirred vessels, Chem. Eng. Sci. 53 (18) (1998) 3269–3280.
[25] A.M. EL-Hamouz, Effect of surfactant concentration and operating temperature on the drop size distribution of silicon oil water dispersion, J. Dispersion Sci. Technol. 28 (5) (2007) 797–804.
[26] D.E. Leng, R.A. Calabrese, Immiscible Liquid-Liquid Dispersions, in: E.L. Paul, V.A. Atiemo-Obeng, S.M. Kresta (Eds.), Handbook of Industrial Mixing, John Wiley & Sons, Inc, 2004, Chapter 12.
[27] A.W. Pacek, S. Chamsart, A.W. Nienow, A. Bakker, The influence of impeller type on mean drop size and drop size distribution in an agitated vessel, Chem. Eng. Sci. 54 (1999) 4211–4222.
[28] K.J. Beck, Mechanisms of drop break-up in stirred vessels using a sawtooth impeller, PhD thesis, School of Mechanical Engineering, Cranfield University, UK, August 1998.
[29] L.A. Cutter, Flow and turbulence in a stirred tank, AIChE J. 12 (1966) 35–44.
[30] J. Costes, J.P. Couderc, Study of laser Doppler anemometry of the turbulent flow induced by Rushton turbine in stirred tank: influence of the size of the units-I. Mean flow and turbulence, Chem. Eng. Sci. 43 (1988) 2751–2764.
[31] H. Wu, G.K. Patterson, Laser Doppler measurements of turbulent-flow parameters in a stirred mixer, Chem. Eng. Sci. 44 (1989) 2207–2221.
[32] G. Zhou, S.M. Kresta, Impact of tank geometry on the maximum turbulence energy dissipation rate for impellers, AIChE J. 42 (9) (1996) 2476–2490.
[33] G. Zhou, S.M. Kresta, Distribution of energy between convective and turbulent flow for three frequently used impellers, Trans. IChemE 74 (1996) 379.
[34] M.C. Ruiz, P. Lermanda, R. Padilla, Drop size distribution in a batch mixer under breakage conditions, Hydrometallurgy 63 (2002) 65–74.
[35] J. Baldyga, J.R. Bourne, A.W. Pacek, A. Amanullah, A.W. Nienow, Effects of agitation and scale up on drop size turbulent dispersions: allowance of intermittency, Chem. Eng. Sci. 56 (2001) 3377–3385.
[36] A. Lam, A.N. Sathyagal, S. Kumar, D. Ramkrishna, Maximum stable drop diameter in stirred dispersions, AIChE J. 42 (1996) 1547–1552.
[37] E.G. Chatzi, C.J. Boutris, C. Kiparissides, On-line monitoring of drop size distribution in agitated vessels. 1: Effects of temperature and impeller speed, Ind. Eng. Chem. Res. 30 (1991) 536–543.
[38] E.G. Chatzi, A.D. Gavrielides, C. Kiparissides, Generalized model for prediction of the steady-state drop size distributions in batch stirred vessels, Ind. Eng. Chem. Res. 28 (1989) 1704–1711.